Macromolecules

ARTICLE

pubs.acs.org/Macromolecules

Hydrogen-Bond-Directed Formation of Supramolecular Polymers Incorporating Head-to-Tail Oriented Dipolar Merocyanine Dyes

Ralf Schmidt, Matthias Stolte, Matthias Grüne, and Frank Würthner*

Institut für Organische Chemie and Röntgen Research Center for Complex Material Systems, Universität Würzburg,
Am Hubland, 97074 Würzburg, Germany

S Supporting Information

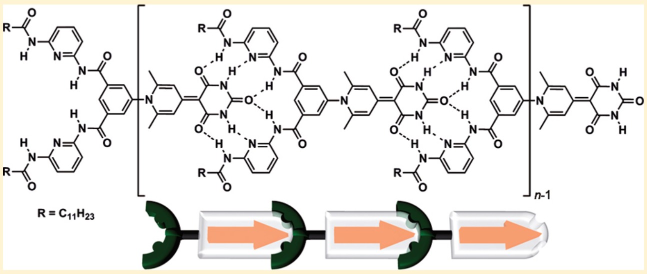

ABSTRACT: A self-complementary Hamilton-receptor-functionalized merocyanine dye has been synthesized by incorporating a hydrogen bonding receptor site to the donor moiety of a merocyanine chromophore that bears a barbituric acid acceptor unit. The optical and electro-optical properties of monomeric dyes have been studied by UV—vis, fluorescence, and electro-optical absorption spectroscopy in chloroform, 1,4-dioxane, tetrahydrofuran, and dimethyl sulfoxide under dilute condition. The self-assembly properties of this self-complementary merocyanine in solution have been investigated by concentration- and temperature-dependent UV—vis and one- and two-dimensional NMR spectroscopy. These studies revealed that the present merocyanine dyes self-assemble in a head-to-tail fashion by forming six hydrogen bonds. The size of the assemblies in solution was determined by dynamic light scattering and diffusion-ordered spectroscopy NMR investigations. In nonpolar solvent mixtures at high concentrations, this merocyanine dye forms appreciably fluorescent gels ($\Phi_{fl} = 0.17$) while the monomeric dye and self-assemblies in solution are only weakly fluorescent ($\Phi_{fl} = 0.07$).

INTRODUCTION

For anisotropic dipolar molecules such as merocyanines, usually the mutual antiparallel orientation in dimeric aggregates is favored by electrostatic interactions.[1] This characteristic property of merocyanine dyes has been used to create supramolecular polymers by tethering two dyes via a spacer unit.[2,3] Hydrogen-bonding interactions, in turn, have been extensively used for creating supramolecular polymers and several reviews have been published on this topic.[4] Hamilton receptors have been employed in various systems for molecular recognition,[5] complexes enabling photoinduced electron-transfer studies,[6] supramolecular polymers,[7] supramolecular dendrimers,[6b,8] foldamers,[9] noncovalently cross-linked block copolymers,[10] and binding of barbiturates to surfaces.[11] Structurally related systems based on melamines were used to arrange merocyanine dyes via hydrogen bonds and afforded a variety of complex architectures.[12] Formation of supramolecular sheet aggregates from self-complementary bis(acylaminopyridines) was also reported.[13]

The question arises whether antiparallel orientation of merocyanine dyes can be circumvented and supramolecular polymers of such dipolar dyes can be achieved by their head-to-tail orientation through hydrogen bonding. Recently, we have shown that the antiparallel arrangement of merocyanines can be overcome in hydrogen-bonded bimolecular complexes of Hamilton-receptor-functionalized merocyanines containing a *N*-alkyl-substituted barbiturate acceptor moiety and complementary merocyanines bearing a barbituric acid unit.[14] Two methyl substituents at the ortho positions of the dihydropyridone heterocycles of the merocyanine dye enforce an almost perpendicular orientation of the two planes of the Hamilton receptor and the chromophore. Thereby, the antiparallel aggregation of the even more dipolar bimolecular complex is impeded.[14] On the basis of this concept, it appears feasible that self-complementary, hydrogen-bonding receptor containing merocyanines would lead to supramolecular polymers by head-to-tail orientation of the dipolar dyes. Therefore, we have constructed the self-complementary merocyanine dye **1** that consists of a Hamilton receptor and a merocyanine chromophore bearing a barbituric acid acceptor group, and studied in detail the self-assembly properties of dye **1** (Scheme 1).

Highly directional noncovalent interactions such as hydrogen bonding are known to facilitate the formation of organogels.[15] Moreover, it has been shown previously that organogels can be prepared from bis(merocyanine) dyes.[2] However, such gels are nonemissive because their supramolecular main chain is based on antiparallel dimer aggregates of these dipolar chromophores which exhibit H-type excitonic coupling of their transition dipole moments. Strong quenching of the fluorescence is well-established for such H-type dimer aggregates,[16] and theoretical interpretations for such quenching have been discussed in the literature.[17] Nevertheless, some exceptions of weakly emissive H-aggregates are known in the literature that are rationalized by rotational offsets of the transition dipole moments or coupling

Received: February 22, 2011
Revised: April 11, 2011
Published: May 02, 2011

Scheme 1. Concept for the Hydrogen-Bond-Directed Formation of Supramolecular Polymers Consisting of Self-Complementary Merocyanine Dyes 1 Arranged in a Head-to-Tail Fashion and Schematic Representation of the Orientation of Dipole Moments upon Self-Assembly

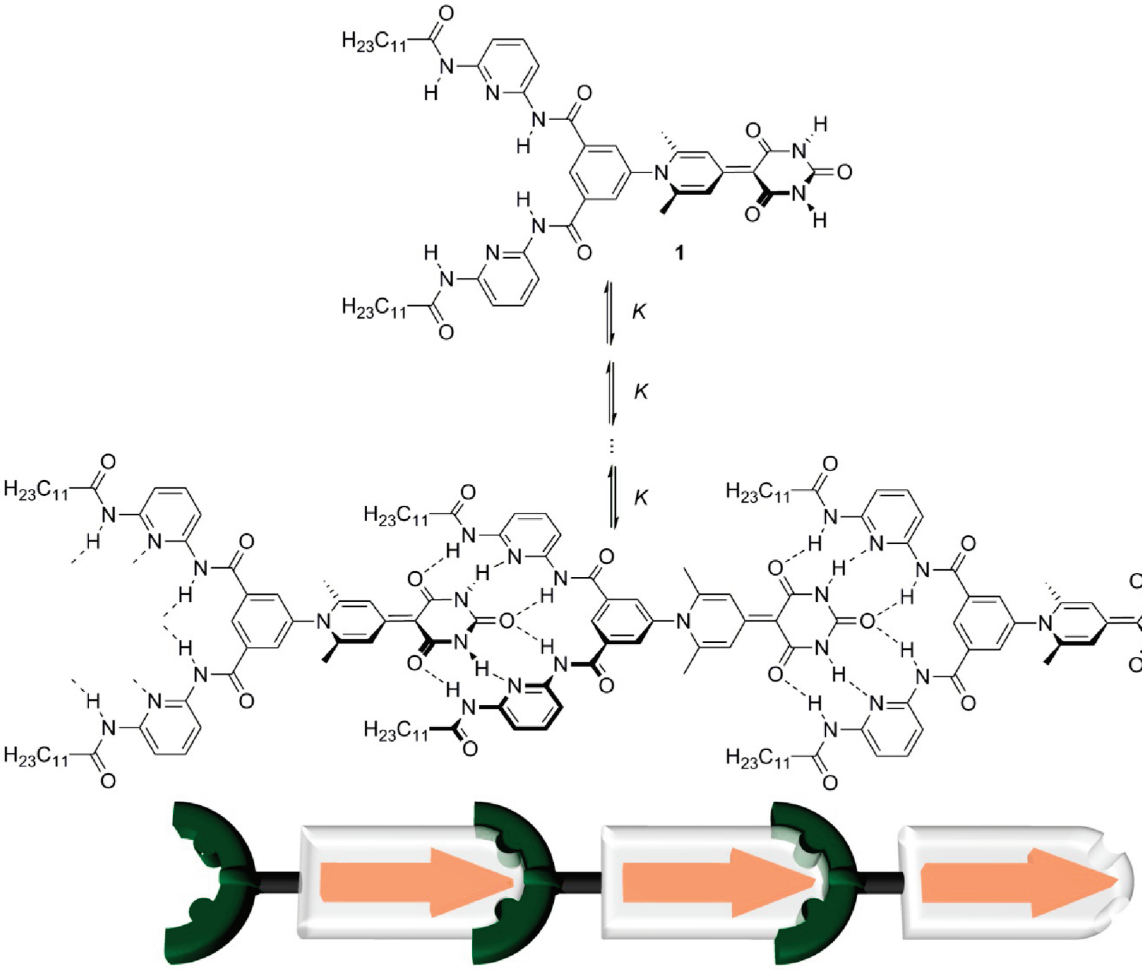

of the (forbidden) lowest energy excitonic transition to molecular vibrations.[12b,18] Organogels based on hitherto unknown hydrogen-bond-mediated merocyanine dye assemblies with head-to-tail arrangement of the dipolar chromophores are good candidates for achieving more favorable emission properties owing to a more suitable orientation of their transition dipole moments. Therefore, we have also investigated the gelation properties of Hamilton-receptor-functionalized merocyanine dye **1** and elucidated their fluorescence properties at the different hierarchies of self-assembly.

■ RESULTS AND DISCUSSION

Synthesis. The Hamilton-receptor-functionalized merocyanine dye **1** was synthesized according to the route outlined in Scheme 2. Diamide **7** was prepared according to the literature, starting with the reaction of 5-aminoisophthalic acid **2** and dehydroacetic acid **3** to pyridone hydrochloride **4**.[14] Esterification of the latter resulted in diethyl ester derivative **5**, which could be transformed to diamide **7** with monolithiated 2,6-diaminopyridine.[14] Subsequent acylation of **7** with dodecanoyl chloride afforded the precursor **8** for the target compound **1** in 42% yield. The Knoevenagel condensation reaction of **8** with CH-acidic barbituric acid **9** yielded the desired Hamilton-receptor-functionalized merocyanine dye **1** in 4%. The low yield of the last step can partially be attributed to the demanding purification process, comprising successive column chromatography, gel permeation chromatography (GPC), and recrystallization. Merocyanine dye guest molecule **10** equipped with a barbituric acid acceptor group, reference Hamilton receptor **11** and Hamilton-receptor-functionalized merocyanine **12** with *n*-butyl substituents in imide positions were prepared according to the literature (structures are shown in Chart 1).[14,19] Merocyanine **12** is a valuable reference system as it is, in contrast to newly synthesized merocyanine **1**, not self-complementary. The precursor **8** and the target compound merocyanine **1** were characterized by NMR spectroscopy (see the Supporting Information, Figures S1, S2) and high-resolution mass spectrometry (HRMS, see Supporting Information, Figures S3, S4), and for **1** MALDI-TOF mass spectrum has also been measured (Supporting Information, Figure S5). For the detailed structural assignment of monomeric dye **1** by 1-D and 2-D NMR spectroscopy, see the section Structural Elucidation by NMR Spectroscopy and the Supporting Information (Table S1).

Spectroscopic Studies of Merocyanine 1 Monomers. In order to investigate the optical and electro-optical properties of

Scheme 2. Synthesis of Self-Complementary Hamilton-Receptor-Functionalized Merocyanine Dye 1

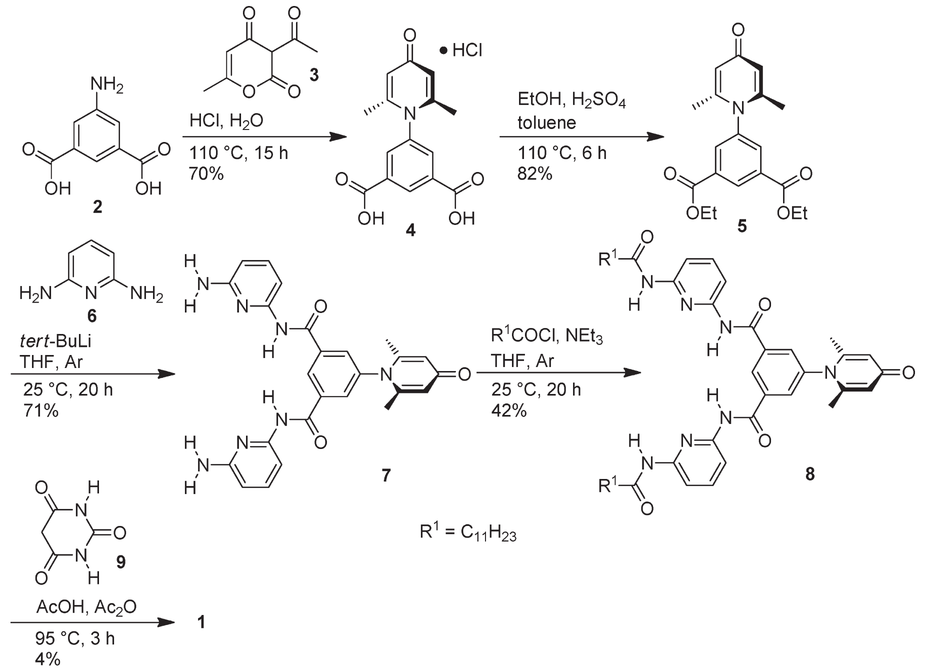

Chart 1. Structures of Merocyanine Dye Guest Molecule 10 Bearing a Barbituric Acid Acceptor Group, Reference Hamilton Receptor 11 and Hamilton-Receptor-Functionalized Merocyanine 12

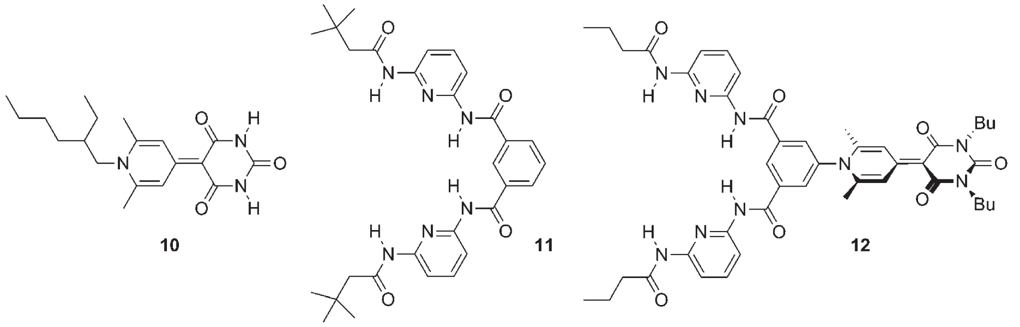

monomers of merocyanine dye **1**, solvents of high polarity like dimethyl sulfoxide (DMSO, ε_r = 46.5) and solvents of strong hydrogen bond acceptor capability like 1,4-dioxane (ε_r = 2.25) were used. The investigation of monomers of **1** in nonpolar solvents is hampered by self-assembly of this self-complementary system. The presence of monomers in deuterated DMSO was confirmed by ^{1}H NMR spectroscopy (for details, see NMR section). Highly dilute solutions were employed to ensure the presence of monomers in 1,4-dioxane ($c = 5.3 \times 10^{-7}$ M)[20] and $CHCl_3$ ($c = 1.4 \times 10^{-7}$ M, T = 328 K). Merocyanine **1** is existent as monomer in highly diluted $CHCl_3$ solution at elevated temperature as was attested by temperature-dependent fluorescence experiments (for details, see fluorescence section). The UV–vis spectra of **1** in 1,4-dioxane, $CHCl_3$, and DMSO exhibit typical absorption properties of monomeric merocyanine dyes. The intense charge transfer (CT) absorption band shows negative solvatochromism as this band is hypsochromically shifted with increasing solvent polarity (λ_{max}(1,4-dioxane) = 396 nm, λ_{max}($CHCl_3$) = 392 nm, λ_{max}(DMSO) = 389 nm) and the absorption coefficient ε is decreased in more polar solvent (Figure 1). This solvatochromism may be attributed to differences in the stabilization of the ground and excited states by the solvent, and hence to the change of the dipole moment difference $\Delta\mu = \mu_e - \mu_g$ (μ_e and μ_g denote the excited and ground state dipole moments, respectively) upon optical excitation in solvents of different polarity.[21,22]

Dipole moments of the ground state μ_g and the dipole moment differences $\Delta\mu$ of merocyanine dye **1**, and the reference compounds **10** and **12** in dilute 1,4-dioxane solution were determined by electro-optical absorption (EOA) spectroscopy.[23,24] A quantitative evaluation of the optical and electro-optical data of these chromophores provides the dipole moments μ_g, transition dipole moment μ_{eg}, and $\Delta\mu$ (Table 1). Only minor differences of the CT absorption bands of merocyanine dyes **1**, **10**, and **12** could be observed (see also Figure S6 in the Supporting Information). The data shown in Table 1 reveal that the covalent attachment of a Hamilton receptor to the donor moiety of the merocyanine chromophore leads to a

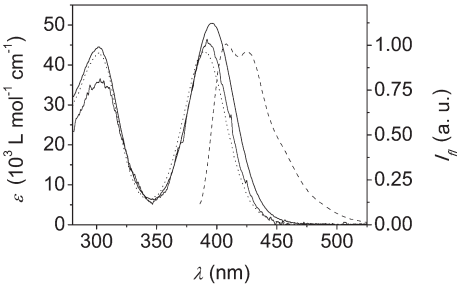

Figure 1. UV−vis absorption spectra of monomeric **1** in 1,4-dioxane (black solid line, 298 K), $CHCl_3$ (gray solid line, 328 K), and DMSO (black dotted line, 298 K) and normalized fluorescence spectrum in $CHCl_3$ (gray dashed line, 328 K, λ_{ex} = 370 nm).

Table 1. Dipole Moments and Optical Data of 1, 10, and 12 Determined by UV−vis and EOA Spectroscopy in 1,4-Dioxane at 298 K[a]

	λ_{max} (nm)	ε_{max} (M^{-1} cm^{-1})	μ_{eg} (D)	μ_g[b] (D)	$\Delta\mu$[b] (D)
10	379	50600	6.5	10.1 ± 0.1	−3.9 ± 0.1
12	391	56000	7.2	7.7 ± 0.1	−3.7 ± 0.1
1	396	50800	6.9	7.9 ± 0.2	−4.3 ± 0.4

[a] Values for compounds **10** and **12** are taken from ref 14a. [b] "Gas phase" dipole moments were calculated by a solvent correction within the approximations of Onsager's continuum model.[24] (1 D = 3.336 × 10^{-30} C m).

bathochromic shift of the absorption maximum (λ_{max}) and an increase of the transition dipole moment (μ_{eg}). The dipolar character of the merocyanine decreases upon attachment of the Hamilton receptor which is attributed to the partial dipole moments of the Hamilton receptor subunit.[25] However, the dipole difference $\Delta\mu$ remains almost unaffected. The negative $\Delta\mu$ values of these merocyanines are in accordance with the observation of negative solvatochromism and are in accordance with recent EOA investigations of bimolecular complex **10:12** which have revealed the formation of hydrogen-bond-mediated highly dipolar structures.[14] Thus, self-complementary Hamilton-receptor-functionalized merocyanine dye **1** constitutes a building block for the creation of self-assembled linear polymers bearing merocyanine dyes in the main chain as suggested in Scheme 1.

Self-Assembly Studies. First indication for the self-assembly of Hamilton-receptor-functionalized merocyanine dyes **1** in the gas phase was obtained by mass spectrometry. Mass peaks observed in MALDI-TOF spectra of dye **1** correspond to monomeric (*m/z* 944.2 ($[M]^+$); calcd. 943.5) and dimeric (*m/z* 1888.1 ($[M_2]^+$); calcd. 1888.3) species (see Supporting Information, Figure S5). To gain insight into the self-assembly properties of self-complementary merocyanine dye **1** in solution, concentration- and temperature-dependent UV−vis spectroscopic studies were performed. Owing to the low solubility of **1** in 1,4-dioxane, no solutions of high concentration could be prepared. Therefore, tetrahydrofuran (THF) was chosen for self-assembly studies since for the formation of the structurally related bimolecular complex **10:12** similar binding constants were found in 1,4-dioxane and THF.[14] The concentration-dependent measurements in THF at 298 K reveal a hypsochromic shift of the absorption maximum upon increasing the concentration (Figure 2a). The observation of an isosbestic point indicates an equilibrium between free and bound dye molecules **1**. Monomeric and self-assembled species may be distinguished on the basis of their absorption maxima at λ_{max} = 396 and 382 nm, respectively. The absorption maxima of free and bound species were extrapolated using eqs 1 and 2 (vide infra). A hypsochromic shift was observed upon self-assembly at high concentrations that can be ascribed to an effect exerted by the receptor which is similar to that of solvents of different polarity on a solvatochromic dye.[14b,21,22] Similar absorption spectral changes were observed for the formation of bimolecular complexes between reference compounds **10** and **11**.[14]

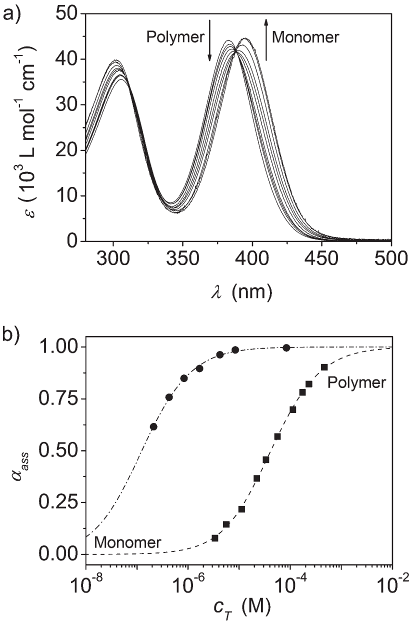

Figure 2. (a) Concentration-dependent UV−vis spectra of **1** in THF at 298 K at the concentration range from $c = 4.7 \times 10^{-4}$ M to 3.4×10^{-6} M. Arrows indicate spectral changes upon dilution. (b) Fraction of associated species α_{ass} in THF (■, calculated from the apparent absorption coefficient ε at 370 nm) and $CHCl_3$ (●, calculated from the apparent absorption coefficient at 375 nm) plotted against c_T and the fitting curves obtained by the nonlinear regression analysis based on the isodesmic model.

The isodesmic model[26] could be applied to the formation of supramolecular polymers from self-complementary dyes **1**. According to this model, the molar fraction of associated species α_{ass} can be expressed as a function of the total concentration c_T and the equilibrium constant K[26]

$$\alpha_{ass} = 1 - \frac{2Kc_T + 1 - \sqrt{4Kc_T + 1}}{2K^2c_T^2} \qquad (1)$$

α_{ass} can be calculated from the apparent absorption coefficient of the solution $\varepsilon(c_T)$ and the absorption coefficients of monomer ε_{mon} and assembly ε_{ass}

$$\alpha_{ass} \approx \frac{\varepsilon(c_T) - \varepsilon_{mon}}{\varepsilon_{ass} - \varepsilon_{mon}} \qquad (2)$$

The equilibrium constant K is defined according to:

$$1_n + 1 \rightleftharpoons 1_{n+1}; \qquad K = \frac{[1_{n+1}]}{[1_n][1]} \qquad (3)$$

Nonlinear regression analysis of the data obtained from the concentration-dependent UV−vis measurements in THF at certain wavelengths by employing eq 1 yielded an equilibrium constant of $K = (1.6 \pm 0.3) \times 10^4$ M^{-1} (Figure 2b). The equilibrium constant was averaged over the values deduced at four different wavelengths (see Supporting Information, Figure S7).

Similar concentration-dependent UV−vis experiments in $CHCl_3$ at 298 K revealed a more pronounced driving force of **1** toward self-assembly (Figure 2b, for more details see Supporting Information, Figures S8 and S9). Hence, it was not possible to cover the whole binding isotherm with data points. Nevertheless, the equilibrium constant in $CHCl_3$ could be roughly estimated to 6.2×10^6 M^{-1}. This value is in good agreement with that for the formation of bimolecular complex **10:12** from reference merocyanines **10** and **12** in $CHCl_3$. For this complex, an equilibrium constant of $K_{dim} > 10^6$ M^{-1} was obtained from ^{1}H NMR titration experiments at a constant host concentration and 298 K.[14]

Temperature-dependent UV−vis measurements in THF revealed spectral changes that are in good accordance with the concentration-dependent series. The self-assembly of **1** was probed upon variation of temperature from 10 to 60 °C in steps of 5 °C at a concentration of $c = 3.5 \times 10^{-5}$ M (see Supporting Information, Figure S10a). A decrease of the temperature resulted in a hypsochromic shift of the absorption maximum, suggesting self-assembly of **1**. The equilibrium between free and bound species is indicated by an isosbestic point. Since, in comparison to the concentration-dependent series, only a smaller part of the transition region from monomeric to polymeric species can be covered within the accessible temperature range (Supporting Information, Figure S10b), the extrapolation of the absorption maxima of free and bound species according to eqs 4 and 5 (vide infra) is less precise. However, the maximum values for monomeric and self-assembled compound at λ_{max} = 396 and 385 nm, respectively, are in reasonable agreement.

The isodesmic self-assembly process was confirmed by an excellent fit of the temperature-dependent isodesmic model[27] (see Supporting Information, Figure S10b). This model expresses the molar fraction of associaated species $\alpha_{ass}(T)$ as a function of temperature[27]

$$\alpha_{ass}(T) = \frac{1}{1 + e^{-0.908\Delta H[(T - T_m)/RT_m^2]}} \qquad (4)$$

where T_m denotes the melting temperature of the assembly and ΔH the molar enthalpy of assembly formation. $\alpha_{ass}(T)$ can be obtained from absorption spectra using the following equation

$$\alpha_{ass}(T) \approx \frac{\varepsilon(T) - \varepsilon_{mon}}{\varepsilon_{ass} - \varepsilon_{mon}} \qquad (5)$$

Application of this model to the apparent absorption coefficients $\varepsilon(T)$ at 395 nm provided T_m = 316 K, the molar Gibbs free energy $\Delta G° = -26.6$ kJ mol^{-1}, and the molar enthalpy of Hamilton complex formation $\Delta H° = -46.2$ kJ mol^{-1} as well as the change of entropy $\Delta S° = -65.8$ J mol^{-1} K^{-1} (see Supporting Information, Table S2). Comparison of the enthalpy and entropy contributions to the total Gibbs free energy changes for association reveals that the self-assembly process is entropically disfavored but enthalpy driven. The equilibrium constant as a function of the temperature was calculated to $K = 4.5 \times 10^4$ M^{-1} at 298 K (see Supporting Information, Figure S10d). It is noteworthy that, in order to investigate the hydrogen-bond-directed association process by UV−vis spectroscopy, conditions were applied where only monomers up to small oligomers are present.

The average of the two equilibrium constants determined from concentration- and temperature-dependent UV−vis experiments in THF was calculated to $K = 3.1 \times 10^4$ M^{-1}, and this value is in very good agreement with the dimerization constant of reference merocyanines **10** and **12** ($K_{dim} = 3.6 \times 10^4$ M^{-1}).[14b] Linear free energy relationships (LFERs) were previously applied to estimate the equilibrium constant in solvents of low polarity.[21,28] With such LFER analysis, a K value in the order of 10^{15} M^{-1} was estimated for the self-assembly of dye **1** in pure *n*-hexane (see Supporting Information, Figure S11 and Table S3). Thus, while under dilute conditions applied in our UV−vis studies in polar solvents only small oligomers are formed, the thermodynamic data suggest the formation of extended supramolecular polymers at higher concentration and in less polar environments.

Structural Elucidation of Monomeric and Self-Assembled Dye 1 by NMR Spectroscopy. The structural binding motif of assemblies of **1** was studied in detail by NMR spectroscopy at a concentration of 0.5 mmol L^{-1} (Figure 3). In the ^{1}H NMR spectrum of **1** in deuterated dimethylsulfoxide (DMSO-d_6), a simple pattern of sharp signals was observed, indicating that dye **1** is monomerically dissolved in this polar solvent. Upon changing the solvent to $CDCl_3$, significant changes compared

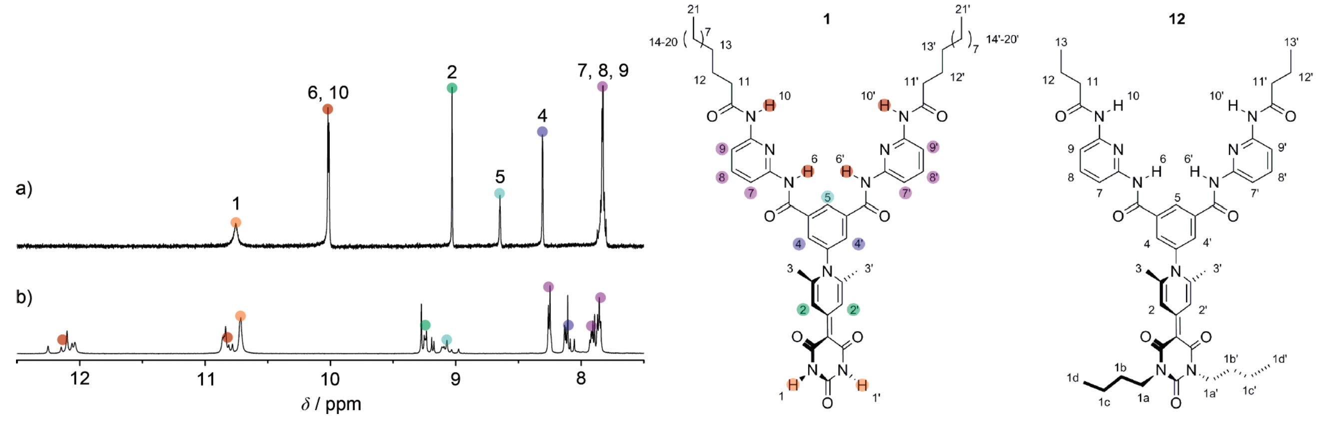

Figure 3. Sections of the ^{1}H NMR spectra of **1** in (a) DMSO-d_6 ($c = 5.0 \times 10^{-4}$ M, 400 MHz, 300 K) and (b) $CDCl_3$ ($c = 5.0 \times 10^{-4}$ M, 600 MHz, 293 K). The colored dots highlight the splitting of selected monomer signals upon self-assembly in $CDCl_3$.

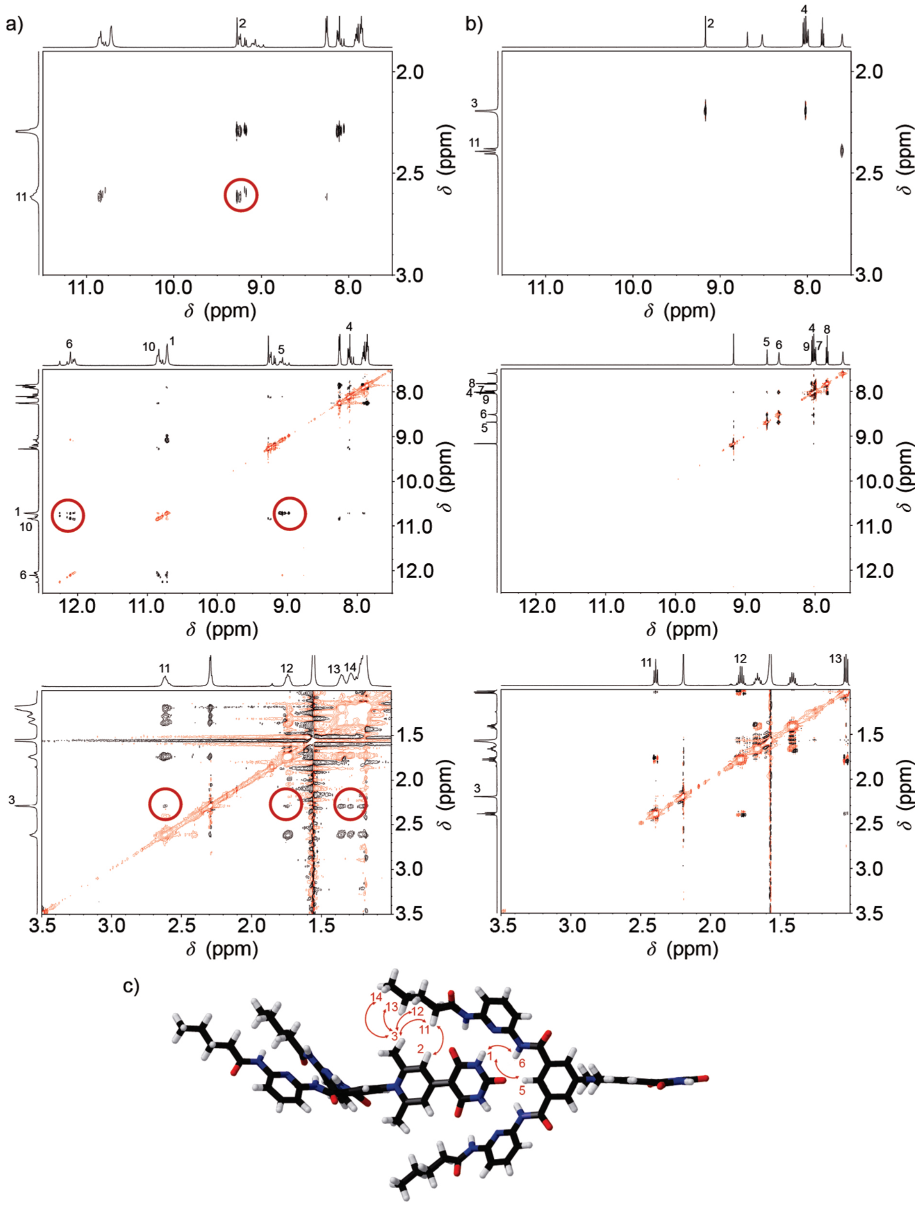

Figure 4. Sections of the 600 MHz ROESY NMR spectra of dyes **1** (a) and **12** (b) in $CDCl_3$ ($c = 5.0 \times 10^{-4}$ M) at 293 K and 250 ms mixing time. Positive and negative signals are represented by black and red lines, respectively. Red circles highlight selected intermolecular cross-coupling peaks. (c) ROESY cross-coupling signals (highlighted by red circles in a) that indicate spatial proximities between the respective protons were implemented in a structural model for a dimer of **1** obtained by molecular modeling on semiempirical level (AM1, HyperChem 8.05[30]). The long alkyl chains in the Hamilton receptor are replaced by butyl groups for simplicity.

to the spectrum in DMSO-d_6 were observed, apparently due to self-assembly. Structural features of the self-assembled species were elucidated by (^{1}H,^{1}H)-COSY, (^{1}H,^{13}C)-HSQC, and (^{1}H,^{13}C)-HMBC NMR experiments (Figure 4). For comparison, similar NMR data were acquired for the reference Hamilton-receptor-functionalized merocyanine **12** in $CDCl_3$ which cannot form self-assemblies owing to *N*-alkyl substituents of the barbiturate acceptor moiety. The complete assignment of the ^{1}H NMR signals is given in Table S1 in the Supporting Information.

Monomers of **1** in DMSO-d_6 showed a single set of nicely resolved ^{1}H NMR signals (Figure 3). The protons marked with and without prime (see the structures in Figure 3) are chemically equivalent, which is in accordance with an overall C_{2v}-symmetry of monomeric **1**. The different conformers of the Hamilton receptor in solution are usually not observable due to fast interconversion on the NMR time scale.[9c] Apart from solvent-induced shifts of signals, a similar pattern was obtained for monomeric reference compound **12** in $CDCl_3$ (see Supporting Information, Table S1).

A considerably more complex spectrum was obtained for supramolecular polymers of **1** in $CDCl_3$. The signals are broader and split into intricate patterns compared to those of monomeric **1** in DMSO-d_6. The splitting for selected proton signals in $CDCl_3$ is highlighted in Figure 3 by dots of the same color. Upon complex formation with a barbituric acid the Hamilton receptor becomes fixed in a specific conformation that deviates from planarity by about 45°.[25] Self-assembly into extended oligomers and the loss of symmetry due to deviation from planarity lead to

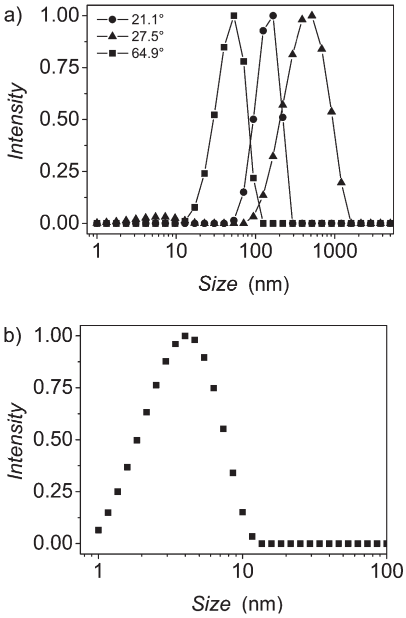

Figure 5. (a) Size distribution of self-assembled **1** at 293 K in $CHCl_3$ ($c = 4.5 \times 10^{-4}$ M) obtained from DLS at different scattering angles indicated in the inset (no evaluable autocorrelation function was obtained for 90°). (b) Size distribution for a mixture of **10**, **1**, and **11** in the ratio of 1:3:1 ($c(\mathbf{1}) = 9.5 \times 10^{-4}$ M, 293 K) measured at 90°.

signal splitting and broadening. In addition, changes of the chemical shifts for protons at positions 5 (0.39 ppm) and 11 (0.23 ppm), and even more for the amide protons 6 (3.60 ppm) and 10 (3.22 ppm), upon self-assembly of **1** could be observed by comparing the ^{1}H NMR data of **1** and **12** in $CDCl_3$ (see Supporting Information, Table S1). Similar shifts have recently been reported for bimolecular complexes of merocyanine **10** with reference Hamilton receptor **11** and merocyanine **12**, respectively,[14] which indicates the formation of self-assemblies of **1** in $CDCl_3$.[29]

The close proximity of protons of two molecules should result in through-space coupling, which can be investigated by rotating-frame Overhauser enhancement spectroscopy (ROESY) NMR. Thus, ROESY experiments were performed with merocyanine **1** and reference compound **12** in $CDCl_3$ at a concentration of 5.0×10^{-4} M. Through-space couplings between the protons of **1** at positions 1 and 6, 1 and 5, 2 and 11, as well as between 3 and 11, 12, 13, and 14 are observed and highlighted by red circles in Figure 4a. All these couplings are in accordance with the geometry-optimized dimer structure (AM1, HyperChem 8.05[30]) of **1** shown in Figure 4c, and thus provide evidence for the Hamilton-receptor-mediated self-assembly of **1** in $CDCl_3$. On the basis of the calculated dimer of **1**, the intermolecular distances between the pairs of protons that show cross-peaks in the ROESY spectrum are well within the range of such experiments, while the intramolecular distances between the respective protons are far beyond the sensitivity of this technique. According to the structure shown in Figure 4c the distance between protons 1 and 10 is short enough to expect through-space couplings in the ROESY spectrum of **1** in $CDCl_3$. However, due to signal splitting and broadening in the assembly, the ^{1}H peaks of these protons partially overlap. Therefore, the region with possible cross peaks between 1 and 10 is excluded from the analysis.

In contrast to the observation of intermolecular cross peaks for **1**, only intramolecular couplings are observed for reference compound **12** for which signals between protons 2 and 3, 3 and 4, 4 and 6, 5 and 6, 7 to 9, and the protons within the respective alkyl chain can be found (Figure 4b).

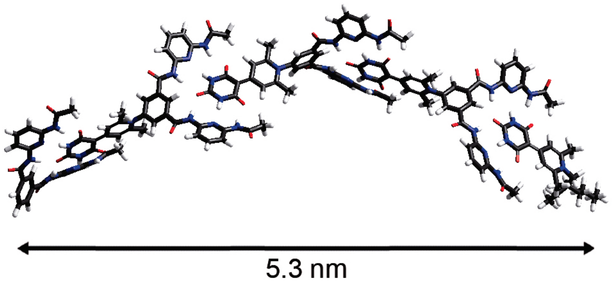

Figure 6. Geometry-optimized (AM1, HyperChem 8.05[30]) structure of complex **10:1$_3$:11**. Long alkyl chains were replaced by methyl groups.

Size of the Assemblies in Solution. Dynamic light scattering (DLS) experiments were performed to determine the size of head-to-tail self-assembled merocyanine dyes **1** in solution. For these studies, we applied a concentration of 4.5×10^{-4} M of **1** in $CHCl_3$ that according to the thermodynamic parameters obtained by UV/vis spectroscopy should afford a degree of polymerization (DP_N) of about 53. DLS measurements revealed average particle sizes from 53 to 516 nm, depending on the scattering angle (Figure 5a and for autocorrelation functions, see Supporting Information, Figure S12). The dependence of the particle size on the scattering angle provides strong evidence for the nonspherical nature of the assemblies. The relatively broad distribution of particle sizes from ~13 to 1606 nm supports the formation of supramolecular polymers. Further evidence for the formation of extended hydrogen-bonded supramolecular polymers was obtained by diffusion-ordered spectroscopy (DOSY) NMR experiments with *DP* (degree of polymerization) values of ~21 at a concentration of 5.0×10^{-4} M at 293 K (for further details see the Supporting Information, Figure S13).

Addition of merocyanine dye **10** and receptor **11** to a solution of **1** in $CHCl_3$ should result in oligomeric self-assemblies of smaller size because these molecules act as chain stoppers.[31] Indeed, DLS of a mixture of **10**, **1**, and **11** in a ratio 1:3:1 in $CHCl_3$ ($c(\mathbf{1}) = 1.0 \times 10^{-4}$ M) at 293 K revealed a significantly decreased average particle size of only 4.3 nm (Figure 5b). Molecular modeling of complex **10:1$_3$:11** on semiempirical level (AM1, HyperChem 8.05[30]) revealed a bended structure with a length of 5.3 nm (Figure 6), which is in good accordance with the value estimated by DLS investigations. The observed narrow size distribution is indicative for the formation of a well-defined oligomeric complex instead of supramolecular polymers.

Gelation and Morphology Study. Gelation tests for dye **1** were conducted in different organic solvents and solvent mixtures. No gel formation could be observed in polar solvents with hydrogen bond acceptor ability like DMSO and THF. In nonpolar aromatic solvent like toluene, precipitation was observed upon cooling the solution to room temperature, while this dye is not soluble in aliphatic solvents like *n*-hexane, even at elevated temperature. In $CHCl_3$/*n*-hexane mixtures with more than 70 vol % of $CHCl_3$ the compound remained dissolved and in solvent mixtures with less than 40 vol % $CHCl_3$ precipitation was observed. Only in a very narrow range, that is, $CHCl_3$/*n*-hexane (40:60 vol %) at 88 mM concentration, a yellow opaque gel was formed at room temperature within 30 min after addition of appropriate amounts of *n*-hexane to a stock solution of **1** in $CHCl_3$ (see Figure 10, inset). The critical gel concentration was found to be 8 wt %.

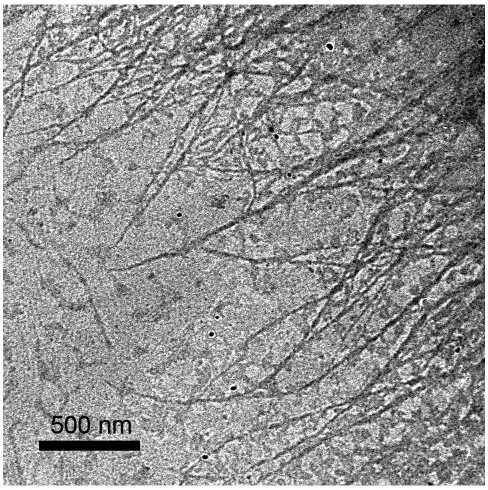

Figure 7. Transmission electron micrograph of self-assembled **1** (c = 2.3 × 10^{-4} M, $CHCl_3$) after evaporation of the solvent on a carbon-coated copper grid.

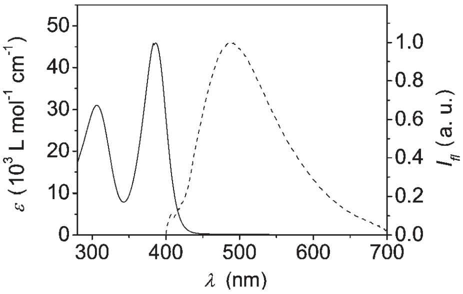

Figure 8. UV−vis absorption and fluorescence spectra (λ_{ex} = 370 nm) of assemblies of merocyanine dye **1** in $CHCl_3$ (c = 0.7 × 10^{-4} M, 298 K).

Once the self-assembly of Hamilton-receptor-functionalized merocyanine dye **1** in solution and its gelation in nonpolar solvent mixtures at high concentrations have been confirmed, the morphology of the assemblies was investigated by transmission electron microscopy (TEM). TEM micrographs show long strands which extend over several micrometers (Figure 7). Their average diameter being ∼14−18 nm is much larger than expected for single fibrils from molecular modeling (see Supporting Information, Figure S14), indicating that individual supramolecular polymers of **1** merge to strands, which further form entangled networks.

Fluorescence Properties. To get information on the impact of supramolecular organization on the fluorescence properties of merocyanine dye **1**, we have carried out fluorescence studies at different concentrations and temperatures. To avoid any influence of the solvent on the emission properties (wavelength, quantum yield), which can be substantial, all investigations were carried out in $CHCl_3$. Like for other common merocyanine dyes,[32] only a very weak fluorescence could be observed for solutions of monomeric dye **1** in $CHCl_3$. To ensure the presence of monomers, these measurements were carried out at low concentrations and elevated temperature (c = 1.4 × 10^{-7} M, 328 K). The maximum of the emission band λ_{em} was observed at 408 nm (see Figure 1) and the fluorescence quantum yield was Φ_{fl} = 0.03. The low-fluorescence quantum yield can be attributed to rapid nonradiative deactivation pathways through a bond-twisting mechanism and constitutes a common feature of merocyanine and cyanine dyes in solution.[33]

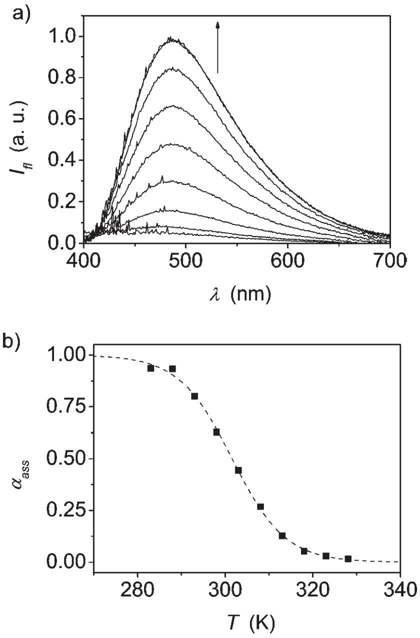

Figure 9. (a) Temperature-dependent fluorescence spectra of **1** in $CHCl_3$ (c = 1.4 × 10^{-7} M, λ_{ex} = 370 nm) from 10 to 55 °C in steps of 5 °C. The arrow indicates changes upon decreasing temperature. (b) Plot of the temperature-dependent molar fractions of self-assembled species α_{ass} calculated from the integrated fluorescence intensity and fitting curve obtained by nonlinear regression analysis based on the isodesmic model.

The emission property of **1** is markedly affected by the formation of head-to-tail supramolecular polymers. Concentrated solutions of **1** in $CHCl_3$ (c = 0.7 × 10^{-4} M, α_{ass} = 1) showed increased emission (Φ_{fl} = 0.07) at λ_{em} = 489 nm (Figure 8) in comparison to that of monomers (Φ_{fl} = 0.03). Excitation spectra ensured that the emission originates from the self-assembled species (see Supporting Information, Figure S15). The increase of the emission might be ascribed to the loss of radiationless deactivation pathways upon self-assembly owing to the rigidification of the molecules upon self-assembly. Several polymethine dyes have been reported to exhibit enhanced emission intensities after being physically or chemically rigidified.[34]

Temperature-dependent fluorescence spectra of merocyanine **1** at low concentration (c = 1.4 × 10^{-7} M, α_{ass} ≈ 0.5 at room temperature) in $CHCl_3$ revealed an increase of the emission with decreasing temperature (Figure 9a). The fluorescence quantum yield increases from Φ_{fl} = 0.03 to 0.07 upon decreasing the temperature from 55 to 10 °C. This increase of fluorescence should be attributed to a transformation of monomers at high temperatures to self-assembled oligomers at low temperatures. The temperature-dependent isodesmic model (vide supra) was applied to a plot of the molar fractions of self-assembled species α_{ass} against the temperature (Figure 9b). From this plot the thermodynamic parameters T_m, K, $\Delta G°$, $\Delta H°$, and $\Delta S°$ for the self-assembly of merocyanine **1** could be obtained (Table 2). α_{ass} was calculated with eq 5 using the integrated fluorescence intensity instead of absorption. With a value of 7.3 × 10^6 M^{-1}, the equilibrium constant is in very good agreement with the value obtained from concentration-dependent UV−vis experiments (K = 6.2 × 10^6 M^{-1}).

Table 2. Thermodynamic Parameters T_m (K), $\Delta G°$ (kJ mol^{-1}), $\Delta H°$ (kJ mol^{-1}), $\Delta S°$ (J mol^{-1} K^{-1}), and K (M^{-1}) Obtained From the Temperature-Dependent Self-Assembly of 1 ($c = 1.4 \times 10^{-7}$ M, CHCl$_3$) Based on the Isodesmic Model

T_m	$\Delta G°$	$\Delta H°$	$\Delta S°$	K[a]
302	−39.2	−137	−131	7.3×10^6

[a] Value determined at 298 K.

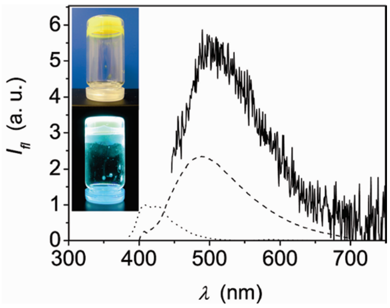

Figure 10. Fluorescence spectrum of a gel prepared from merocyanine **1** in CHCl$_3$/*n*-hexane (40:60 vol %, c = 88 mM, λ_{ex} = 370 nm, solid line) and of monomeric ($c = 1.4 \times 10^{-7}$ M, 328 K, λ_{ex} = 370 nm, dotted line) and self-assembled ($c = 0.7 \times 10^{-4}$ M, λ_{ex} = 370 nm, dashed line) dye **1** in CHCl$_3$. The inset shows a photograph of the gel at ambient conditions and the fluorescence upon excitation with UV light (λ_{ex} = 366 nm).

The gel phase of merocyanine dyes **1** showed a remarkably intense bluish-white fluorescence emission (Figure 10). In comparison to the monomeric (Φ_{fl} = 0.03) and self-assembled species (Φ_{fl} = 0.07), the fluorescence of the gel is significantly increased (Φ_{fl} = 0.17) and shifted to slightly longer wavelengths (λ_{em} = 496 nm). The modest shift corroborates our earlier conclusion that the individual dyes remain isolated by means of the sterical shielding of the bulky and orthogonally arranged Hamilton receptors (see Scheme 1). No indication for the formation of excimers as observed for antiparallel dimer aggregates of related dipolar merocyanine dyes[18] is obtained from the emission spectra of the self-assembled species of merocyanine **1** shown in Figure 10. These results demonstrate that even such highly dipolar dyes like **1** can be self-assembled by strong 6-fold hydrogen-bonding receptors in a head-to-tail supramolecular polymer without forming quenching sites by close $\pi-\pi$-contacts through dipolar aggregation.

CONCLUSIONS

In this work, the first example of a head-to-tail supramolecular polymer with incorporated merocyanine dyes is reported. Self-complementary Hamilton-receptor-functionalized merocyanine dyes **1** enabled to outwit the most common antiparallel aggregation of the dipolar merocyanine dyes, and hence to achieve the highly desirable head-to-tail orientation of such dyes by 6-fold hydrogen bonding, leading to the formation of supramolecular polymers with appreciable solubility in common organic solvents such as CHCl$_3$ and THF. Evaluation of concentration- and temperature-dependent UV−vis experiments of merocyanine dye **1** by employing the isodesmic model revealed high equilibrium constants for the self-assembly of **1** that gave rise to high degrees of polymerization even in dilute solutions. Our results further revealed that the rigidification of weakly emissive chromophores, in particular merocyanines, in supramolecular polymer networks can afford interesting fluorescent materials as desired for sensory and photonic applications if the design of the supramolecular polymer impedes quenching sites such as $\pi-\pi$-aggregates with H-type excitonic interaction. Future directions of research on such supramolecular polymers may be in the area of electro-optical and nonlinear optical applications where desired polarizability anisotropies and second order nonlinear optical effects arise from the orientation of dipolar molecules and/or assemblies in external electric fields.[35] Other applications may give rise to light emitting devices or sensory systems. The enhanced emission properties of the supramolecular polymers and gel phase in comparison to the nearly nonemissive monomer are particularly promising in this regard.

EXPERIMENTAL SECTION

Materials and Methods. Solvents and reagents were acquired from commercial suppliers and used without further purification, unless otherwise stated. THF was dried according to literature.[36] Column chromatography was performed using silica gel (Merck Silica 60, particle size 0.04−0.063 nm). Thin layer chromatography (TLC) was performed on silica gel plates (60 F$_{254}$ Merck, Darmstadt). Gel permeation chromatography (GPC) was carried out on a recycling preparative LC-9105 system (Japan Analytical Industries Co., Ltd.) with a UV−vis (UV-3702, 380 nm) and a refractive index detector (RI-7s) using a preparative JAIGEL-1H+2H column and solvents of purity grad “pa”. Determination of the melting points (uncorrected) was conducted on a Büchi Melting Point B545 heating stage. Solvents for UV−vis absorption and AFM studies were of spectroscopic grade and used as received. Unless otherwise stated, ^{1}H NMR spectra were recorded on a Bruker Avance 400 spectrometer at 300 K with TMS or residual undeuterated solvent as internal standard. MALDI-TOF mass spectrometry was performed on an autoflex II instrument (Bruker Daltronik GmbH) in positive mode with a DCTB matrix. A microTOF focus instrument (Bruker Daltronik GmbH) was used to perform high resolution ESI-TOF mass spectrometry in positive mode with CH$_3$CN and CHCl$_3$ or THF and CHCl$_3$ as solvent.

UV−vis Experiments. UV−vis absorption spectra were recorded on a Perkin-Elmer Lambda 950 UV−vis spectrophotometer with a spectral bandwidth of 0.20 nm and a scan rate of 141 nm/min. Conventional quartz cells of 0.1−50 mm path length were used to cover a suitable concentration range. Temperature control was achieved with a PTP-1 Peltier element (Perkin-Elmer).

Fluorescence Measurements. The steady-state fluorescence spectra in solution were recorded under ambient conditions on a PTI QM4/2003 spectrofluorometer. A front-face setup was used for the self-assembled solution in CHCl$_3$ owing to the high optical density of the sample. All fluorescence spectra were corrected against photomultiplier and lamp intensity. Because of the overlap of the excitation peak with the emission, the excitation peak was removed by subtraction of a spectrum of the pure solvent. The fluorescence quantum yields were determined using the optical dilution method with diphenylanthracene (Φ_{fl} = 0.67 in benzene[37]) as standard.[38] The given quantum yields are averaged over the values obtained at three different excitation wavelengths. Absolute quantum yields of the gel were measured under ambient conditions on an absolute photoluminescence quantum yield measurement system C9920-02 (Hamamatsu).

Dynamic Light Scattering (DLS). DLS experiments were carried out using a commercial N5 Submicrometer Particle Size Analyzer (Beckman Coulter, Inc.) laser light scattering spectrometer equipped with a 25 mW helium−neon laser operating at 632.8 nm. Sample solutions (c(**1**) = 1.0×10^{-4} M) were filtrated into a dust-free vial through a 0.45 μm Teflon filter. The size distribution profile deconvolution algorithm is based on the CONTIN program.

Gelation Tests. The measured amount of organogelator (merocyanine **1**) was dissolved in the respective amount of $CHCl_3$ in a screw-capped sample vial. Gels were formed upon addition of appropriate amounts of *n*-hexane to the stock solution. The formation of the gel was tested by the "stable-to-inversion of a vial" method[39] after leaving the sample for 1 h at ambient conditions.

Synthesis and Characterization of Precursor 8 and the Target Compound 1. *1-{3,5-Bis[(6-dodecyrylamino)pyridine-2-yl]carbamoyl}phenyl-2,6-dimethyl-4-pyridone (**8**).* Diamine **7** (2.22 g, 4.72 mmol) was dissolved in dry THF (140 mL) under an argon atmosphere and cooled to 0 °C. At this temperature, dodecanoyl chloride (2.38 g, 2.59 mL, 10.9 mmol) was added dropwise. Afterward, the reaction mixture was stirred for 16 h at room temperature. The resultant suspension was poured into a saturated aqueous solution of $NaHCO_3$ (200 mL, pH 8−10). After extracting the aqueous layer with $CHCl_3$ (4×50 mL), the combined organic layers were dried over $MgSO_4$. The solvent was removed under reduced pressure and the residue was purified by column chromatography using silica gel with EtOAc/EtOH = 10:1 vol % as eluent to give pure **8** (1.65 g, 1.98 mmol, 42%). ^1H NMR (400 MHz, $CDCl_3$): δ 9.92 (br s, 4 H, NH), 8.86 (s, 1 H, ArH), 8.25 (s, 2 H, ArH), 8.06 (d, $^3J = 7.2$ Hz, 2 H, $CH_{pyridine}$), 8.01 (d, $^3J = 5.9$ Hz, 2 H, $CH_{pyridine}$), 7.77 (t, $^3J = 7.4$ Hz, 2 H, $CH_{pyridine}$), 2.33 (t, $^3J = 7.2$ Hz, 4 H, $COCH_2$), 1.77 (s, 6 H, CH_3), 1.67 (m, 4 H, CH_2), 1.23 (m, 32 H, CH_2), 0.86 (t, $^3J = 6.8$ Hz, 6 H, CH_3). ^{13}C NMR (ca. 100 MHz, $CDCl_3$): δ 172.59, 163.18, 150.64, 149.78, 140.87, 139.49, 136.93, 130.29, 117.53, 117.07, 116.93, 116.88, 110.66, 110.31, 37.63, 34.46, 32.03, 29.34, 25.50, 25.10, 21.83, 14.23. HRMS (ESI, pos. mode, $CH_3CN/CHCl_3$ = 1:1 vol %): calc. *m*/*z* $C_{49}H_{68}N_7O_5$ ($[M + H]^+$) 834.52819; found 834.52764.

*5-{1-[3,5-Bis[(6-dodecyrylamino)pyridine-2-yl]carbamoyl]phenyl-2,6-dimethyl-pyridine-4-ylidene}-pyrdimidine-2,4,6-trione (**1**).* A catalytic amount of concentrated HOAc was added to a solution of pyridone **8** (1.77 g, 2.12 mmol) and barbituric acid **9** (272 mg, 2.12 mmol) in Ac_2O (3.80 mL). The resultant reaction mixture was heated to 90 °C for 3 h. Afterward the solvent was removed under reduced pressure. In a first purification step, the crude product was purified by column chromatography using silica gel and CH_2Cl_2/MeOH = 98.5:1.5 vol %. Subsequent purification by GPC ($CHCl_3$) and repeated reprecipitation from $CHCl_3$/*n*-hexane yielded pure **1** (80.1 mg, 84.8 μmol, 4%). Mp 325−327 °C (decomposition). UV/vis (1,4-dioxane): λ_{max}/nm (ε_{max}/L mol^{-1} cm^{-1}) = 396 (50.8×10^3). ^1H NMR (400 MHz, 293 K, DMSO-d_6): δ 10.75 (s, 2 H, NH), 10.02 (s, 4 H, NH), 9.03 (s, 2 H, CH), 8.65 (s, 1 H, ArH), 8.31 (s, 2 H, ArH), 7.83 (m, 6 H, $CH_{pyridine}$), 2.39 (t, $^3J = 7.7$ Hz, 4 H, $COCH_2$), 2.22 (s, 6 H, CH_3), 1.58 (m, 4 H, CH_2), 1.24 (m, 32 H, CH_2), 0.85 (t, $^3J = 6.8$ Hz, 6 H, CH_3). ^{13}C NMR (ca. 150 MHz, 313 K, DMSO-d_6): δ 172.00, 170.57, 170.39, 165.12, 165.09, 163.77, 150.43, 150.03, 149.98, 139.83, 136.18, 129.94, 129.49, 123.46, 113.54, 110.03, 109.99, 36.02, 31.10, 30.76, 24.47, 24.83, 21.90, 21.88, 21.86, 13.72. HRMS (ESI, pos. mode, $CHCl_3$/THF = 1:1 vol %): calc. *m*/*z* $C_{53}H_{70}N_9O_7$ ($[M+H]^+$) 944.53927; found 944.53850.

■ ASSOCIATED CONTENT

Ⓢ Supporting Information. ^1H NMR spectra of key compounds **1** and **8**, assignment of proton signals of **1** and reference compound **12**, supplementary mass, UV−vis, and fluorescence spectra, detailed data evaluation, and molecular modeling. This material is available free of charge via the Internet at http://pubs.acs.org.

■ AUTHOR INFORMATION

Corresponding Author

*Fax: (+49) 931-31-84756. E-mail: wuerthner@chemie.uni-wuerzburg.de.

■ ACKNOWLEDGMENT

We gratefully thank Dr. Xin Zhang for performing TEM measurements and the Volkswagen Foundation for financial support of this work within the priority program "Complex Materials: Cooperative Projects on the Natural, Engineering and Biosciences".

■ REFERENCES

(1) (a) Würthner, F.; Yao, S. *Angew. Chem., Int. Ed.* **2000**, *39*, 1978–1981. (b) Würthner, F.; Yao, S.; Debaerdemaker, T.; Wortmann, R. *J. Am. Chem. Soc.* **2002**, *124*, 9431–9447.

(2) (a) Würthner, F.; Yao, S.; Beginn, U. *Angew. Chem., Int. Ed.* **2003**, *42*, 3247–3250. (b) Yao, S; Beginn, U.; Gress, T.; Lysetska, M.; Würthner, F. *J. Am. Chem. Soc.* **2004**, *126*, 8336–8348. (c) Lohr, A.; Lysetska, M.; Würthner, F. *Angew. Chem., Int. Ed.* **2005**, *44*, 5071–5074. (d) Lohr, A.; Gress, T.; Deppisch, M; Knoll, M; Würthner, F. *Synthesis* **2007**, 3073–3082.

(3) (a) Schmidt, R.; Uemura, S.; Würthner, F. *Chem.—Eur. J.* **2010**, *16*, 13706–13715. (b) Yagai, S.; Nakano, Y.; Seki, S.; Asano, A.; Okubo, T.; Isoshima, T.; Karatsu, T.; Kitamura, A.; Kikkawa, Y. *Angew. Chem., Int. Ed.* **2010**, *49*, 9990–9994.

(4) (a) Sherrington, D. C.; Taskinen, K. A. *Chem. Soc. Rev.* **2001**, *30*, 83–93. (b) Brunsveld, L.; Folmer, B. J. B.; Meijer, E. W.; Sijbesma, R. P. *Chem. Rev.* **2001**, *101*, 4071–4097. (c) Hoeben, F. J. M.; Jonkheijm, P.; Meijer, E. W.; Schenning, A. P. H. J. *Chem. Rev.* **2005**, *105*, 1491–1546. (d) Binder, W. H.; Zirbs, R. *Adv. Polym. Sci.* **2007**, *207*, 1–78. (e) Shimizu, L. S. *Polym. Int.* **2007**, *56*, 444–452.

(5) Chang, S.-K.; Hamilton, A. D. *J. Am. Chem. Soc.* **1988**, *110*, 1318–1319.

(6) (a) Tecilla, P.; Dixon, R. P.; Slobodkin, G.; Alavi, D. S.; Waldeck, D. H.; Hamilton, A. D. *J. Am. Chem. Soc.* **1990**, *112*, 9408–9410. (b) Dirksen, A.; Hahn, U.; Schwanke, F.; Nieger, M.; Reek, J. N. H.; Vögtle, F.; De Cola, L. *Chem.—Eur. J.* **2004**, *10*, 2036–2047. (c) McClenaghan, N. D.; Grote, Z.; Darriet, K.; Zimine, M.; Williams, R. M.; De Cola, L.; Bassani, D. M. *Org. Lett.* **2005**, *7*, 807–810. (d) Molard, Y.; Bassani, D. M.; Desvergne, J.-P.; Horton, P. N.; Hursthouse, M. B.; Tucker, J. H. R. *Angew. Chem., Int. Ed.* **2005**, *44*, 1072–1075. (e) Wessendorf, F.; Gnichwitz, J.-F.; Sarova, G. H.; Hager, K.; Hartnagel, U.; Guldi, D. M.; Hirsch, A. *J. Am. Chem. Soc.* **2007**, *129*, 16057–16071. (f) Wessendorf, F.; Grimm, B.; Guldi, D. M.; Hirsch, A. *J. Am. Chem. Soc.* **2010**, *132*, 10786–10795.

(7) (a) Berl, V.; Schmutz, M.; Krische, M. J.; Khoury, R. G.; Lehn, J.-M. *Chem.—Eur. J.* **2002**, *17*, 1227–1244. (b) Kolomiets, E.; Buhler, E.; Candau, S. J.; Lehn, J.-M. *Macromolecules* **2006**, *39*, 1173–1181. (c) Binder, W. H.; Petraru, L.; Roth, T.; Groh, P. W.; Pálfi, V.; Keki, S.; Ivan, B. *Adv. Funct. Mater.* **2007**, *17*, 1317–1326.

(8) Franz, A.; Bauer, W.; Hirsch, A. *Angew. Chem., Int. Ed.* **2005**, *44*, 1564–1567.

(9) (a) Zhao, X.; Li, Z.-T. *Chem. Commun.* **2010**, *46*, 1601–1616. (b) Berl, V.; Huc, I.; Khoury, R. G.; Krische, M. J.; Lehn, J.-M. *Nature* **2000**, *407*, 720–723. (c) Berl, V.; Krische, M. J.; Huc, I.; Lehn, J.-M.; Schmutz, M. *Chem.—Eur. J.* **2000**, *6*, 1938–1946.

(10) (a) Binder, W. H.; Bernstorff, S.; Kluger, C.; Petraru, L.; Kunz, M. *Adv. Mater.* **2005**, *17*, 2824–2828. (b) Burd, C.; Weck, M. *Macromolecules* **2005**, *38*, 7225–7230.

(11) (a) Motesharei, K.; Myles, D. C. *J. Am. Chem. Soc.* **1994**, *116*, 7413–7414. (b) Binder, W. H.; Kluger, C.; Josipovic, M.; Straif, C. J.; Friedbacher, G. *Macromolecules* **2006**, *39*, 8092–8101.

(12) (a) Yagai, S.; Higashi, M.; Karatsu, T.; Kitamura, A. *Chem. Mater.* **2005**, *17*, 4392–4398. (b) Yagai, S.; Higashi, M.; Karatsu, T.; Kitamura, A. *Chem. Commun.* **2006**, 1500–1502. (c) Yagai, S.; Kinoshita, T.; Higashi, M.; Kishikawa, K.; Nakanishi, T.; Karatsu, T.; Kitamura, A. *J. Am. Chem. Soc.* **2007**, *129*, 13277–13287.

(13) Ikeda, M.; Nobori, T.; Schmutz, M.; Lehn, J.-M. *Chem.—Eur. J.* **2005**, *11*, 662–668.

(14) (a) Würthner, F.; Schmidt, J.; Stolte, M.; Wortmann, R. *Angew. Chem., Int. Ed.* **2006**, *45*, 3842–3846. (b) Schmidt, J.; Schmidt, R.; Würthner, F. *J. Org. Chem.* **2008**, *73*, 6355–6362.

(15) (a) Terech, P.; Weiss, R. G. *Chem. Rev.* **1997**, *97*, 3133–3159. (b) van Esch, J. H.; Feringa, B. L. *Angew. Chem., Int. Ed.* **2000**, *39*, 2263–2266. (c) Estroff, L. A.; Hamilton, A. D. *Chem. Rev.* **2004**, *104*, 1201–1217. (d) Hirst, A. R.; Smith, D. K. *Chem.—Eur. J.* **2005**, *11*, 5496–5508. (e) Hirst, A. R.; Escuder, B.; Miravet, J. F.; Smith, D. K. *Angew. Chem., Int. Ed.* **2008**, *47*, 8002–8018. (f) Foster, J. A.; Steed, J. W. *Angew. Chem., Int. Ed.* **2010**, *49*, 6718–6724. (f) Ajayaghosh, A.; Praveen, V. K. *Acc. Chem. Res.* **2007**, *40*, 644–656.

(16) (a) Lewschin, W. L. *Z. Phys.* **1927**, *43*, 230–253. (b) Rabinowitch, E.; Epstein, L. *J. Am. Chem. Soc.* **1941**, *63*, 69–78. (c) Förster, T.; König, E. *Z. Elektrochem.* **1957**, *61*, 344–348. (d) Bergmann, K.; O'Konski, C. T. *Z. Phys. Chem.* **1963**, *67*, 2169–2177. (e) West, W.; Pearce, S. *J. Phys. Chem.* **1965**, *69*, 1894–1903.

(17) (a) Förster, T. *Z. Naturwissenschaften* **1946**, *33*, 166–175. (b) Kasha, M.; Rawls, H. R.; El-Bayoumi, M. A. *Pure Appl. Chem.* **1965**, *11*, 371–392.

(18) Rösch, U.; Yao, S.; Wortmann, R.; Würthner, F. *Angew. Chem., Int. Ed.* **2006**, *45*, 7026–7030.

(19) Würthner, F. *Synthesis* **1999**, *12*, 2103–2113.

(20) Solvent-dependent binding studies of reference compounds **10** and **12** revealed slightly lower binding constants in 1,4-dioxane in comparison to those in THF (see ref 14). Since concentration-dependent UV/vis experiments for **1** in THF revealed the predominant existence of monomers at low concentrations, one can safely assume that compound **1** is present in its monomeric state under the conditions applied in this experiment.

(21) Reichardt, C. *Solvents and Solvent Effects in Organic Chemistry*, 3rd ed.; Wiley-VCH: Weinheim, 2002.

(22) Würthner, F.; Archetti, G.; Schmidt, R.; Kuball, H.-G. *Angew. Chem., Int. Ed.* **2008**, *47*, 4529–4532.

(23) (a) Liptay, W. *Excited States*; Lim., E. C., Ed.; Academic Press: New York, 1974; Vol. 1, pp 129—229. (b) Beckmann, S.; Etzbach, K.H.; Krämer, P.; Lukaszuk, K.; Matschiner, R.; Schmidt, A. J.; Schuhmacher, P.; Sens, R.; Seybold, G.; Wortmann, R.; Würthner, F. *Adv. Mater.* **1999**, *11*, 536–541.

(24) (a) Onsager, L. *J. Am. Chem. Soc.* **1936**, *58*, 1486–1493. (b) Böttcher, C. F. J. *Theory of Electric Polarization*, 2nd ed.; Elsevier Scientific Pub. Co.: Amsterdam, 1973.

(25) Stolte, M. Ph.D. thesis, Universität Kaiserslautern, 2008.

(26) (a) Martin, R. B. *Chem. Rev.* **1996**, *96*, 3043–3064. (b) Zhao, D.; Moore, J. S. *Org. Biomol. Chem.* **2003**, *1*, 3471–3491. (c) Chen, Z.; Lohr, A.; Saha-Möller, C. R.; Würthner, F. *Chem. Soc. Rev.* **2009**, *38*, 564–584. (d) De Greef, T. F. A.; Smulders, M. M. J.; Wolffs, M.; Schenning, A. P. H. J.; Sijbesma, R. P.; Meijer, E. W. *Chem. Rev.* **2009**, *109*, 5687–5754.

(27) (a) Smulders, M. M. J.; Nieuwenhuizen, M. M. L.; de Greef, T. F. A.; van der Schoot, P.; Schenning, A. P. H. J.; Meijer, E. W. *Chem.—Eur. J.* **2010**, *16*, 362–367. (b) van der Schoot, P. *Supramolecular Polymers*, 2nd ed.; Ciferri, A., Ed.; CRC Press, Taylor & Francis Group: New York, 2005; pp 77—106.

(28) (a) Schneider, H.-J. *Angew. Chem., Int. Ed.* **1991**, *30*, 1417–1436. (b) Reichardt, C. *Chem. Rev.* **1994**, *94*, 2319–2358. (c) Abraham, M. *Chem. Soc. Rev.* **1993**, *22*, 73–83. (d) Cook, J. L.; Hunter, C. A.; Low, C. M. R.; Perez-Velasco, A.; Vinter, J. G. *Angew. Chem., Int. Ed.* **2007**, *46*, 3706–3709.

(29) It is to note that because the electronic structure of merocyanine dyes, and hence the chemical shift, strongly depends on the solvent polarity,[21] comparison of the NMR data of **1** with those of structurally akin reference compound **12** in $CDCl_3$ seems more appropriate than comparison of data of **1** in $CDCl_3$ and DMSO-d_6 as solvent effects in the latter case cannot be excluded.

(30) *HyperChem* 8.05; Hypercube Inc.: Gainesville, FL.

(31) (a) Sijbesma, R. P.; Beijer, F. H.; Brunsveld, L.; Folmer, B. J. B.; Hirschberg, J. H. K. K.; Lange, R. F. M.; Lowe, J. K. L.; Meijer, E. W. *Science* **1997**, *278*, 1601–1604. (b) Castellano, R. K.; Rudkevich, D. M.; Rebek, J. *Proc. Natl. Acad. Sci. U.S.A.* **1997**, *94*, 7132–7137.

(32) Würthner, F.; Sens, R.; Etzbach, K.-H.; Seybold, G. *Angew. Chem., Int. Ed.* **1999**, *38*, 1649–1652.

(33) (a) Ephardt, H.; Fromherz, P. *J. Phys. Chem.* **1989**, *93*, 7717–7725. (b) Harriman, A. *J. Photochem. Photobiol. A* **1992**, *65*, 79–93. (c) Khairutdinov, R. F.; Serpone, N. *J. Phys. Chem. B* **1997**, *101*, 2602–2610. (d) Karunakaran, V.; Lustres, J. L. P.; Zhao, L.; Ernsting, N. *J. Am. Chem. Soc.* **2006**, *128*, 2954–2962.

(34) Strong enhancement of the fluorescence has been reported for merocyanine dyes upon rigidification in frozen solutions, the solid state, organogels, and polymer films. For some examples, see:(a) Würthner, F.; Sens, R.; Etzbach, K.-H.; Seybold, G. *Angew. Chem., Int. Ed.* **1999**, *38*, 1649–1652. (b) Reference 19. (c) Bondarev, S. L.; Tikhomirov, S. L.; Knyukshto, V. N.; Turban, A. A.; Ishchenko, A. A.; Kulinich, A. V.; Ledoux, I. *J. Lumin.* **2007**, *124*, 178–186.

(35) (a) Würthner, F.; Wortmann, R.; Meerholz, K. *ChemPhysChem* **2002**, *3*, 17–31. (b) Marder, S. R.; Kippelen, B.; Jen, A. K.-Y.; Peyghambarian, N. *Nature* **1997**, *388*, 845–851. (c) Verbiest, T.; Houbrechts, S.; Kauranen, M.; Clays, K.; Persoons, A. *J. Mater. Chem.* **1997**, *7*, 2175–2189. (d) Kanis, D. R.; Ratner, M. A.; Marks, T. J. *Chem. Rev.* **1994**, *94*, 195–242.

(36) Perrin, D. D.; Armarego, W. L. F. *Purification of Laboratory Chemicals*; Pergamon Press: Oxford, 1980.

(37) Heller, C. A.; Henry, R. A.; McLaughlin, B. A.; Bliss, D. E. *J. Chem. Eng. Data* **1974**, *19*, 214–219.

(38) Demas, J. N.; Crosby, G. A. *J. Phys. Chem.* **1971**, *65*, 991–1024.

(39) Low Molecular Mass Gelators. In *Topics in Current Chemistry*; Fages, F., Ed.; Springer: Berlin, 2005; Vol. 256.